

Efficient Proton-Templated Synthesis of 18- to 38-Membered Tetraimino(amino)diphenol Macrocyclic Ligands: Structural Features and Spectroscopic Properties

Bula Dutta,[†] Pradip Bag,[†] Bibhutosh Adhikary,^{†,‡} Ulrich Flörke,[§] and Kamalaksha Nag^{*,†}

Department of Inorganic Chemistry, Indian Association for the Cultivation of Science, Jadavpur, Kolkata 700032, India, and Anorganische und Analytische Chemie, Universität Paderborn, D-33098 Paderborn, Germany

ickn@mahendra.iacs.res.in

Received February 6, 2004

A whole range of Robson-type tetraiminodiphenol macrocyclic ligands have been prepared as their perchlorate salts $[H_4L](ClO_4)_2$ in high yield (ca. 90%) by a single-step $[2 + 2]$ condensation reaction between 4-methyl(or *tert*-butyl)-2,6-diformyl(or diacyl)phenols and α,ω -diaminoalkanes (C_2-C_{12}) in the presence of acetic acid and $NaClO_4$. The reduction of these 18- to 38-membered macrocyclic salts with $NaBH_4$ have afforded corresponding tetraaminodiphenol macrocycles H_2L' . The X-ray crystal structures of two of the tetraiminodiphenol macrocycles with the C_2 and C_4 lateral chains have been determined, and the optimized configurations for all of the macrocycles have been obtained by molecular mechanics calculations. The macrocycles have been characterized by elemental analysis and by IR, absorption, emission, and NMR spectroscopic study. The protonated tetraiminodiphenol macrocycles exhibit strong fluorescence in methanol, acetonitrile, and nitromethane and undergo quenching when treated with triethylamine. The neutral macrocycles H_2L , isolated by treating $[H_4L](ClO_4)_2$ with excess of triethylamine, lack luminescence, as do the reduced tetraaminodiphenol macrocycles H_2L' . The hydrolytic cleavage of $[H_4L](ClO_4)_2$ has been studied.

Introduction

The first reported study¹ on $[2 + 2]$ cyclocondensation reaction between 4-methyl-2,6-diformylphenol and 1,3-diaminopropane in the presence of some divalent metal salts to produce homodinuclear phenoxo-bridged tetraiminodiphenolate macrocyclic complexes has led to numerous studies on related systems.^{2–15} This type of dinuclear complexes, commonly referred to as Robson-type macrocyclic complexes, provides a platform to study

the implications of cooperative metal–metal interactions as manifested in spin exchange couplings,^{6–15} redox activities,^{4,8,9a,11} and bimetallic reactivities.^{9b,16}

The metal-templated route for generating the dinuclear macrocyclic complexes is applicable when the metal ion is labile and in the divalent state. On the other hand, to obtain complexes in which at least one of the metal

[†] Indian Association for the Cultivation of Science.

[‡] Permanent address: Shihpur B.E. College (Deemed University), Howrah, India.

[§] Universität Paderborn.

- (1) Pilkington, N. H.; Robson, R. *Aust. J. Chem.* **1970**, *23*, 2225.
- (2) (a) Okawa, H.; Kida, S. *Inorg. Nucl. Chem. Lett.* **1971**, *7*, 751.
- (b) Okawa, H.; Kida, S. *Bull. Chem. Soc. Jpn.* **1972**, *45*, 1759.
- (3) (a) Hoskins, B. F.; Williams, G. A. *Aust. J. Chem.* **1975**, *28*, 2607.
- (b) Hoskins, B. F.; McLeod, N. J.; Schaap, H. A. *Aust. J. Chem.* **1976**, *29*, 515.
- (4) Addison, A. N. *Inorg. Nucl. Chem. Lett.* **1976**, *12*, 899.
- (5) (a) Gagne, R. R.; Koval, C. A.; Smith, T. J. *J. Am. Chem. Soc.* **1977**, *99*, 8367. (b) Gagne, R. R.; Koval, C. A.; Smith, T. J.; Cimolino, M. C. *J. Am. Chem. Soc.* **1979**, *101*, 4571.
- (6) (a) Spiro, C. L.; Lambert, S. E.; Smith, T. J.; Duesler, E. N.; Gagne, R. R.; Hendrickson, D. N. *Inorg. Chem.* **1981**, *20*, 1229. (b) Long, R. C.; Hendrickson, D. N. *J. Am. Chem. Soc.* **1983**, *105*, 1513.
- (7) (a) Mandal, S. K.; Nag, K. *J. Chem. Soc., Dalton Trans.* **1983**, 2429. (b) Mandal, S. K.; Nag, K. *J. Chem. Soc., Dalton Trans.* **1984**, 2141. (c) Mandal, S.; Adhikary, B.; Nag, K. *J. Chem. Soc., Dalton Trans.* **1986**, 1175.
- (8) (a) Mandal, S. K.; Thompson, L. K.; Nag, K.; Charland, J.-P.; Gabe, E. J. *Inorg. Chem.* **1987**, *26*, 1391. (b) Mandal, S. K.; Thompson, L. K.; Nag, K.; Charland, J.-P.; Gabe, E. J. *Can. J. Chem.* **1987**, *65*, 2815. (c) Mandal, S. K.; Thompson, L. K.; Newlands, M. J.; Gabe, E. J.; Nag, K. *Inorg. Chem.* **1990**, *29*, 1324.

- (9) (a) Zanello, P.; Tamburini, S.; Vigato, P. A.; Mazzocchin, G. A. *Coord. Chem. Rev.* **1987**, *77*, 165. (b) Vigato, P. A.; Tamburini, S.; Fenton, D. E. *Coord. Chem. Rev.* **1990**, *106*, 25. (c) Guerriero, P.; Tamburini, S.; Vigato, P. A. *Coord. Chem. Rev.* **1995**, *139*, 17.
- (10) Lacroix, F.; Kahn, O.; Theobald, F.; Leory, J.; Wakselman, C. *Inorg. Chim. Acta* **1988**, *142*, 129.
- (11) (a) Brychcy, K.; Dragger, K.; Jens, K.-J.; Tilset, M.; Behrens, U. *Chem. Ber.* **1994**, *127*, 465. (b) Brychcy, K.; Jens, K.-J.; Tilset, M.; Behrens, U. *Chem. Ber.* **1994**, *127*, 991. (c) Brychcy, K.; Dragger, K.; Jens, K.-J.; Tilset, M.; Behrens, U. *Chem. Ber.* **1994**, *127*, 1817.
- (12) Thompson, L. K.; Mandal, S. K.; Tandon, S. S.; Bridson, J. N.; Park, M. K.; *Inorg. Chem.* **1996**, *35*, 3317.
- (13) (a) Nanda, K. K.; Thompson, L. K.; Bridson, J. N.; Nag, K. *Chem. Commun.* **1994**, 1337. (b) Nanda, K. K.; Das, R.; Thompson, L. K.; Venkatsubramanian, K.; Paul, P.; Nag, K. *Inorg. Chem.* **1994**, *33*, 1188. (c) Nanda, K. K.; Das, R.; Thompson, L. K.; Venkatsubramanian, K.; Nag, K. *Inorg. Chem.* **1994**, *33*, 5394. (d) Dutta, S. K.; Werner, R.; Flörke, U.; Mohanta, S.; Nanda, K. K.; Haase, W.; Nag, K. *Inorg. Chem.* **1996**, *35*, 2292. (e) Mohanta, S.; Nanda, K. K.; Thompson, L. K.; Flörke, U.; Nag, K. *Inorg. Chem.* **1998**, *37*, 1465.
- (14) Bosnich, B. *Inorg. Chem.* **1999**, *38*, 2557 and references therein.
- (15) (a) Asokan, A.; Verghese, B.; Manoharan, P. T. *Inorg. Chem.* **1999**, *38*, 4393. (b) Mohanta, S.; Adhikary, B.; Baitalik, S.; Nag, K. *New J. Chem.* **2001**, 1466.
- (16) (a) Atkins, A. J.; Blake, A. J.; Schröder, M. *Chem. Soc., Chem. Commun.* **1993**, 353. (b) Atkins, A. J.; Black, D.; Blake, A. J.; Marin-Becerra, A.; Parsons, S.; Rez-Ramirez, L.; Schröder, M. *Chem. Commun.* **1993**, 457. (c) Black, D.; Blake, A. J.; Finn, R. L.; Lindoy, L. F.; Nezhdali, A.; Rougnaghi, G.; Tasker, P. A.; Schröder, M. *Chem. Commun.* **2002**, 340.

centers is in the oxidation state greater than +2 or is kinetically inert, the requirement of preformed macrocyclic ligands become essential.

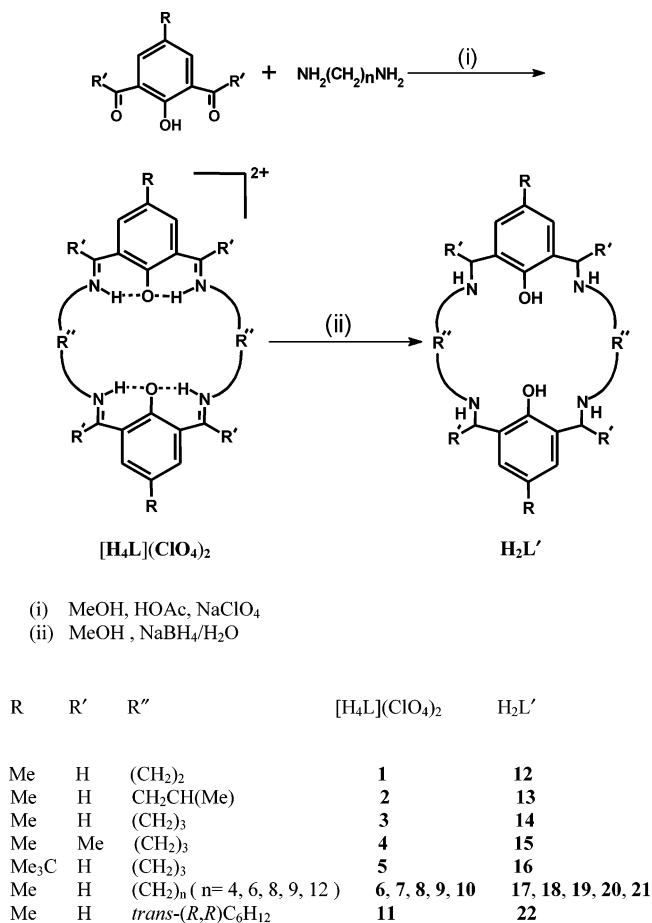
The synthesis of tetraaminodiphenol macrocycles (H_2L) by direct reaction between 2,6-diformyl(or diacyl)phenols and diaminoalkanes is inhibited by uncontrolled oligomerization process. A [3 + 3] cyclocondensation reaction involving 4-methyl-2,6-diformylphenol and *trans*-(*R,R*)-1,2-diaminocyclohexane has been reported to occur under high dilution condition.¹⁷ Again, 1,2-diaminobenzene reacts with 4-methyl-2,6-diformylphenol to produce the partially reduced diiminodiaminodiphenol macrocycle.¹⁸ The synthesis of tetraaminodiphenol macrocycles is additionally affected by the proclivity of hydrolytic cleavage of the azomethine linkages in these compounds. To obviate these problems, Robson et al.¹⁹ adopted a proton-templated approach in which 4-methyl-2,6-diformylphenol was reacted with 1,3-diaminopropane in methanol in the presence of HBr, and the imineprotonated macrocycle was isolated as the bromide salt $[H_4L](Br_3)_2$ after addition of bromine. This bromide salt, however, because of its poor solubility did not turn out to be suitable for complex formation. Subsequently, for the purpose of metal complexation, the bromide salt was converted to the soluble $[H_4L](PF_6)_2$ salt by metathesis.^{16a} In this way a few more tetraaminodiphenol macrocycle derivatives were prepared and their crystal structures were determined.^{16,20} Despite this improvement, the overall yield of the products, however, remained unsatisfactory.

As part of our studies²¹ on mixed-metal, mixed-valent, and higher-valent complexes of tetraimino(or amino)-diphenol macrocycles, we have been motivated to develop an efficient synthetic route that would provide the macrocyclic ligands in high yield. It has been of particular interest to generalize and extend the [2 + 2] cyclocondensation reaction involving 4-methyl(or *tert* butyl)-2,6-diformyl(or diacyl)phenols and α,ω -diaminoalkanes to long chain amines, as the variation of the cavity sizes of the macrocycles is expected to influence host-guest interactions significantly. We report here the synthesis, structural characteristics, and the fluorophoric behavior of the perchlorate salts $[H_4L](ClO_4)_2$ of 18- to 38-membered tetraaminodiphenol macrocycles **1–11** and corresponding neutral tetraaminodiphenol macrocycles (H_2L') **12–22** (shown in Scheme 1).

Result and Discussion

Synthesis. We have reasoned that the success of [2 + 2] cyclocondensation reaction between 4-methyl(or *tert* butyl)-2,6-diformyl(or diacyl)phenols and α,ω -diaminoalkanes, especially for long chain diamines, will depend on

SCHEME 1



several factors. In the first place, to minimize disordered oligomeric condensation the reaction should be carried out under mild condition. Second, to circumvent hydrolytic cleavage of the C=N groups the nitrogen atoms should be protonated to get them involved in hydrogen bonding with the phenolate oxygens and thereby enhance thermodynamic stability of the macrocyclic system. The strength and the amount of the acid to be used for proton-templated condensation is important in this context. We have noted²² that a weak acid such as acetic acid in amount sufficient to supply the required equivalents of H⁺ ion serves remarkably well for this purpose. The third aspect to consider is that a suitable salt should be present in excess in the reaction medium to supply the required counteranions to facilitate in crystallizing out the macrocyclic salt. Finally, the role of solvent is important, and methanol was determined to be the best one.

On the basis of these considerations, we have found that on slow addition of a methanol solution of α,ω -diaminoalkane (1 equiv) to a hot methanol solution containing 4-methyl(or *tert* butyl)-2,6-diformyl(or diacyl)-phenol (1 equiv), acetic acid (2 equiv), and NaClO₄ (4 equiv) the macrocyclic compounds **1–11** (Scheme 1) separate out on standing at room temperature for several hours in 90% yield. The tetraaminodiphenol macrocycles (H_2L') **12–22** (Scheme 1) are readily obtained by reducing their tetraimino derivatives in methanol with NaBH₄.

(22) Dutta, B.; Adhikary, B.; Bag, P.; Flörke, U.; Nag, K. *J. Chem. Soc., Dalton Trans.* **2002**, 2760.

(17) (a) Korupoju, S. R.; Zacharias, P. S. *Chem. Commun.* **1998**, 1267. (b) Korupoju, S. R.; Mangayakarasi, N.; Ameerunisha, S.; Valente, E. J.; Zacharias, P. S. *J. Chem. Soc., Dalton Trans.* **2000**, 2845.

(18) Aguiari, A.; Bullita, E.; Casellato, U.; Guerriero, P.; Tamburini, S.; Vigato, P. A. *Inorg. Chim. Acta* **1992**, *202*, 157.

(19) Hoskins, B. F.; Robson, R.; Williams, G. A. *Inorg. Chim. Acta* **1976**, *16*, 121.

(20) Tian, Y.; Tang, J.; Frenzen, G.; Sun, J.-Y. *J. Org. Chem.* **1999**, *64*, 1442.

(21) (a) Dutta, S. K.; Ensling, J.; Werner, R.; Flörke, U.; Haase, W.; Gültich, P.; Nag, K. *Angew. Chem., Int. Ed. Engl.* **1997**, *36*, 152. (b) Mohanta, S.; Saal, C.; Nag, K.; Dutta, S. K.; Werner, R.; Haase, W.; Duin, E.; Johnson, M. *Ber. Bunsen-Ges.* **1996**, *100*, 2086. (c) Ostovsky, S. M.; Werner, R.; Nag, K.; Haase, W. *Chem. Phys. Lett.* **2000**, *320*, 295.

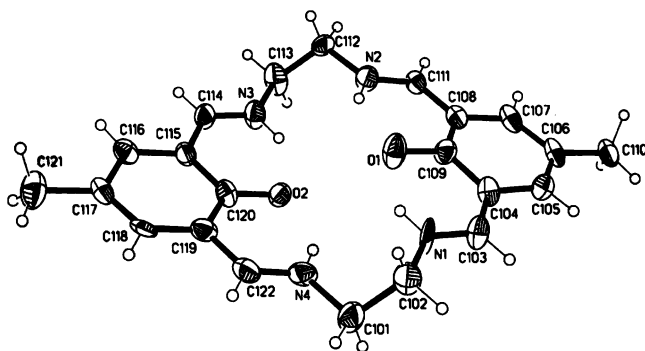


FIGURE 1. ORTEP view of the $[H_4L]^{2+}$ cation of **1**.

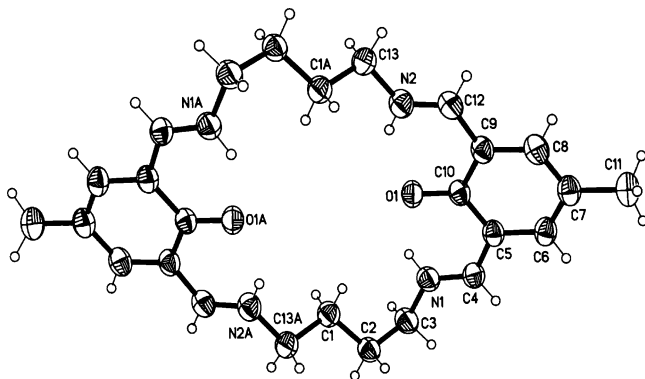


FIGURE 2. ORTEP view of the $[H_4L]^{2+}$ cation of **6**.

The product is isolated from the same reaction pot in 40–60% yield by diluting the methanol solution with water.

Structure. The X-ray crystal structures of the macrocycles **1** and **6** have been determined. In **1**, there are two independent asymmetric units in the unit cell, albeit they have the same structure. In the case of **6**, a crystallographic inversion center is present in the geometric center of the cation. The perchlorate anions in this compound are highly disordered with three oxygen atoms split over two positions each with 0.5 occupancy. The methyl hydrogens also show positional disordering, again split over two positions with 0.5 occupation each.

The ORTEP diagrams along with atom labelings for the $[H_4L]^{2+}$ cations of **1** (for one of the molecules) and **6** are shown in Figures 1 and 2, respectively. The packing diagram of **6** (Figure 3) shows intermolecular stacking. Both compounds **1** and **6** have “stepped” conformation in which the dihedral angle between the phenyl ring planes for the two molecules of **1** are $2.9(1)^\circ$ and $1.9(1)^\circ$, whereas for **6** this angle is zero (as a result of crystallographic symmetry). It may be mentioned that in the case of the hexafluorophosphate salt of **3** the dihedral angle between the planes of the phenyl rings is 14° .¹⁶

The relevant bond distances and angles of the macrocycles **1** and **6**, including the hydrogen bonds involved therein, are given in Table 1. The intramolecular hydrogen bonds involving the phenolic oxygens and the imino nitrogens are of particular importance because the macrocyclic cations $[H_4L]^{2+}$ are stabilized by these bonds. The $N\cdots O$ distances lie in the range 2.54–2.60 Å, while the $N-H\cdots O$ angles vary between 137° and 139° , which indicate that the intramolecular hydrogen bonds are quite strong. There are two ways of depicting the

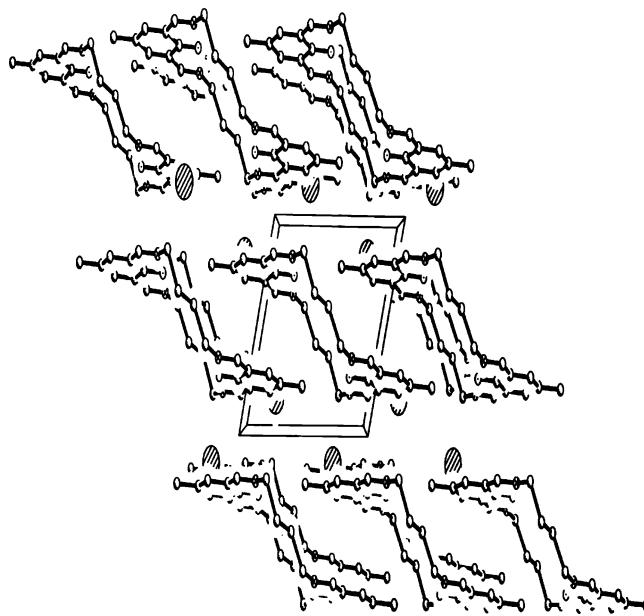


FIGURE 3. Packing diagram of **6** viewed along the c -axis. Perchlorate ions are shown as spheres of arbitrary size.

hydrogen bonds in the $[H_4L]^{2+}$ cation, albeit in both cases the phenolic oxygens will act as bridges. The first possibility to consider is that of the four dissociable protons, two are attached to the oxygens and the remaining two are attached to two of the imino nitrogens. This will lead to an asymmetric $N-H\cdots O-H\cdots N$ type of hydrogen bonding. In the second possibility all protons may be considered to be transferred to the imino nitrogens, resulting in a symmetric $N-H\cdots O\cdots H-N$ type of hydrogen bonding. The second possibility appears to be more reasonable because in the final Fourier difference map weak electron density peaks (due to hydrogens) were observed at shorter distance from N but at longer distance from O. Moreover, the 1H NMR spectra of the macrocycles (see later) also show the presence of a single peak due to the hydrogen-bonded protons, indicating it to be the symmetric type.

The minimum energy configurations of all of the macrocyclic compounds have been obtained by semiempirical AM1²³ and PM3²⁴ calculations.²⁵ The structural parameters obtained from PM3 calculations are in better agreement with those obtained from X-ray crystallography. The optimized structures of **1–11** are shown in Figure 4, and those of **12–22** (shown in Figure S1) are available as Supporting Information.

The geometric configurations of the tetraaminodiphenol macrocycles (H_2L') (Figure S1) show that for this class of compounds, unlike their predecessors $[H_4L](ClO_4)_2$, intramolecular hydrogen bondings have no significant role in defining their structures. Indeed, all four $N\cdots O$ distances in each of these compounds are unequal, and throughout the series they vary in the range 2.7–3.9 Å. The following are heats of formation (ΔH) of the two series of macrocyclic compounds in their gaseous state,

(23) Dewar, M. J. S.; Zoebisch, E. G.; Healy, E. F.; Stewart, J. J. P. *J. Am. Chem. Soc.* **1985**, *107*, 3902.

(24) Stewart, J. J. P. *J. Comp. Chem.* **1989**, *10*, 209.

(25) MOPAC, version 5.0; Cambridge Soft Corporation: Cambridge, USA.

TABLE 1. Selected Bond Lengths (Å) and Angles (deg) for 1 and 6

compound 1					
molecule 1		molecule 2		compound 6	
N (1)–C (103)	1.272 (13)	N (5)–C (203)	1.312 (14)	N (1)–C (4)	1.285 (5)
N (2)–C (111)	1.279 (13)	N (6)–C (211)	1.302 (14)	N (2)–C (12)	1.287 (5)
N (3)–C (114)	1.275 (13)	N (7)–C (214)	1.258 (14)	N (1)–C (3)	1.468 (5)
N (4)–C (122)	1.298 (15)	N (8)–C (222)	1.299 (14)	N (2)–C (13)	1.462 (5)
N (1)–C (102)	1.448 (14)	N (5)–C (202)	1.472 (15)	O (1)–C (10)	1.288 (5)
N (2)–C (112)	1.460 (13)	N (6)–C (212)	1.479 (14)	N (1)–O (1)	2.584 (5)
N (3)–C (113)	1.473 (14)	N (7)–C (213)	1.465 (14)	N (2)–O (1)	2.595 (5)
N (4)–C (101)	1.484 (15)	N (8)–C (201)	1.434 (15)		
O (1)–C (109)	1.295 (12)	O (3)–C (209)	1.276 (12)		
O (2)–C (120)	1.298 (12)	O (4)–C (220)	1.287 (12)		
N (1)–O (1)	2.565 (12)	N (5)–O (3)	2.567 (12)		
N (2)–O (1)	2.541 (12)	N (6)–O (3)	2.540 (12)		
N (3)–O (2)	2.569 (12)	N (7)–O (4)	2.536 (12)		
N (4)–O (2)	2.546 (11)	N (8)–O (4)	2.582 (12)		
N (1)–C (103)–C (103)	122.8 (11)	N (5)–C (203)–C (204)	121.1 (11)	N (1)–C (4)–C (5)	122.5 (4)
N (2)–C (111)–C (108)	121.9 (11)	N (6)–C (211)–C (208)	120.5 (11)	N (2)–C (12)–C (9)	122.1 (4)
N (3)–C (114)–C (115)	123.4 (11)	N (7)–C (214)–C (215)	123.3 (12)	C (4)–N (1)–C (3)	126.1 (4)
N (4)–C (122)–C (119)	121.0 (12)	N (8)–C (222)–C (219)	123.4 (11)	C (12)–N (2)–C (13)	126.5 (4)
C (103)–N (1)–C (102)	129.1 (10)	C (203)–N (5)–C (202)	127.6 (11)	N (1)–C (3)–C (2)	110.5 (4)
C (111)–N (2)–C (112)	126.9 (10)	C (211)–N (6)–C (212)	124.3 (10)	N (2)–C (13)–C (1#)	109.3 (3)
C (114)–N (3)–C (113)	127.4 (10)	C (214)–N (7)–C (213)	126.7 (11)	N (1)–H–O (1)	137.0
C (122)–N (4)–C (101)	125.5 (10)	C (222)–N (8)–C (201)	128.8 (11)	N (2)–H–O (1)	137.8
N (1)–C (102)–C (101)	114.8 (10)	N (5)–C (202)–C (201)	108.1 (11)		
N (2)–C (112)–C (113)	113.5 (10)	N (6)–C (212)–C (213)	109.1 (11)		
N (3)–C (113)–C (112)	110.5 (10)	N (7)–C (213)–C (212)	112.8 (11)		
N (4)–C (101)–C (102)	109.6 (10)	N (8)–C (201)–C (202)	111.2 (11)		
N (1)–H–O (1)	138.9	N (5)–H–O (3)	138.7		
N (2)–H–O (1)	138.3	N (6)–H–O (3)	137.6		
N (3)–H–O (2)	137.7	N (7)–H–O (4)	136.7		
N (4)–H–O (2)	138.9	N (8)–H–O (4)	138.5		

as obtained from PM3 calculations. $[\text{H}_4\text{L}](\text{ClO}_4)_2$: 355 (1), 341 (2), 332 (3), 291 (4), 302 (5), 311 (6), 284 (7), 261 (8), 242 (9), 210 (10), 322 (11) kcal mol⁻¹. $\text{H}_2\text{L}'$: -62 (12), -72 (13), -65 (14), -88 (15), -101 (16), -80 (17), -101 (18), -126 (19), -138 (20), -169 (21), -87 (22) kcal mol⁻¹.

The lowering of ΔH values indicates more relaxed configurations of the compounds. As expected, for both of the series of compounds their heat of formation decreases monotonically with the increase of the lateral alkyl chain lengths. Interestingly, the magnitude of difference in the heats of formation between a $[\text{H}_4\text{L}](\text{ClO}_4)_2$ compound and its corresponding $\text{H}_2\text{L}'$ derivative lie in the range 400 ± 20 kcal mol⁻¹ for the entire series of compounds. Clearly, the reduction of a tetraimino macrocycle to its tetraamino analogue leads to the release of almost 400 kcal mol⁻¹.

Spectroscopy. All of the macrocyclic compounds have been characterized by IR, UV-vis absorption, emission, and NMR (¹H, ¹³C, COSY, DEPT) spectroscopic measurements. The IR spectra of the macrocycles $[\text{H}_4\text{L}](\text{ClO}_4)_2$ exhibit characteristic bands due to $\nu_{\text{C}=\text{N}}$ at ca. 1650 cm⁻¹ (for 4, 1625 cm⁻¹) and at ca. 1100 and 625 cm⁻¹ due to ClO_4^- . Significantly, no bands due to either ν_{NH} or ν_{OH} are observed for these compounds in the range 3500–3000 cm⁻¹. It seems likely that as a result of strong hydrogen bonding the N–H–O–H–N vibrations are shifted to still lower energies and the intensities are also attenuated to get lost in the CH stretching region (3000–2800 cm⁻¹). By contrast, the macrocycles $\text{H}_2\text{L}'$ exhibit two bands at 3340–3310 and 3270–3260 cm⁻¹ due to ν_{NH} and $\nu_{\text{OH(phenol)}}$, respectively. Further, the NH bending vibration is observed at 1610 cm⁻¹.

The ¹H NMR spectra of the macrocycles 1–11 were obtained in CD₃CN and (CD₃)₂SO, and those of 12–22

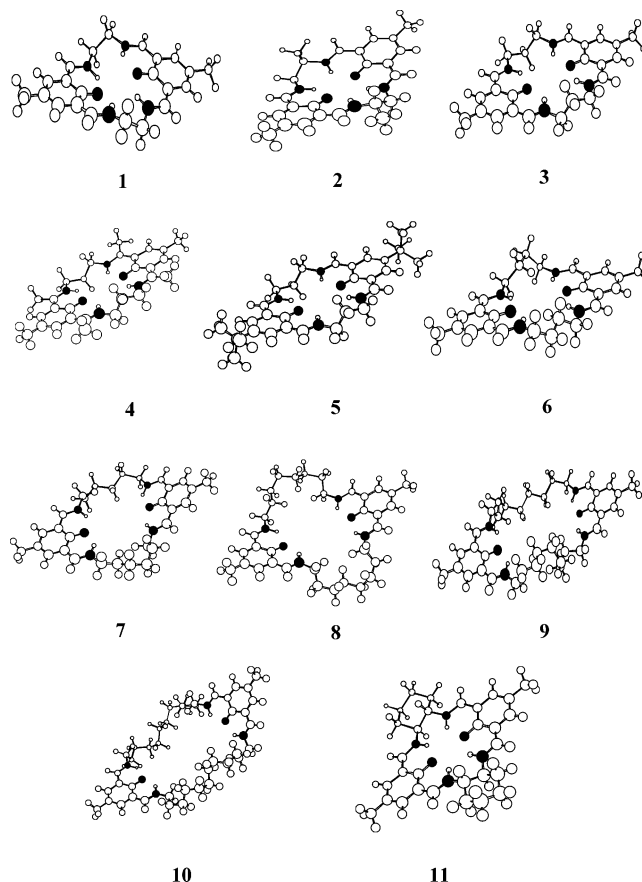


FIGURE 4. Optimized structures of compounds 1–11. The filled circles indicate the imino nitrogens and phenolic oxygens.

in CDCl₃. The spectral features observed for the [H₂L]-(ClO₄)₂ type of compounds, except that of **2**, are quite similar in the aromatic region. They exhibit a somewhat broad singlet in the range 13–15 ppm indicating the equivalency of all four hydrogen-bonded protons. In the case of **2**, this signal is split into four equal components (Figure S2). For this compound, two geometrical isomers with their lateral chain methyl groups in *cis* and *trans* positions are expected. Moreover, because of chirality their *RR/SS* and *RS/SR* diastereoisomers should be also present. Thus, splitting of the hydrogen-bonded signal into four components signifies the occurrence of all of the stereoisomers in equal amount. The CH=N resonance in compounds **1**, **3**, and **5–11** are observed in the range 8.35–8.65 ppm either as a singlet or as a doublet due to weak coupling with the hydrogen-bonded proton ($J = \text{ca. } 13 \text{ Hz}$). In the case of **2**, this particular resonance is observed as four lines. Again, the phenyl ring protons of **2** are observed as a closely spaced multiplet as against a singlet (7.3–7.8 ppm) for the other members of the series. In the aliphatic region, although the chemical shift due to the methyl group is almost the same (ca. 2.3 ppm) for all the compounds, the number and positions of the CH₂ resonances vary for these compounds. The ¹H NMR spectra of **2**, **7**, and **9** (Figure S2–S4) are available as Supporting Information.

The reduced macrocycles **12–22** do not show any low field resonance beyond 7 ppm, indicating the absence of intramolecular hydrogen bonding. The spectral features exhibited by **12**, **14**, and **17–21** have very much in common with the chemical shifts due to the singlets of the aromatic (ca. 6.75 ppm), Ar-CH₂ (ca. 3.82 ppm), and CH₃ (ca. 2.20 ppm) protons. Owing to the presence of multiple chiral centers, the spectral features of **13**, **15**, and **22** are more complex in nature. For example, compound **15**, which has four chiral centers, exhibits (Figure S5) 4-line singlets due to the aromatic protons and 8-line features for both Ar-C*H-CH₃ protons. The spectra observed for **19** and **21** (Figures S6 and S7), the compounds with C₉ and C₁₂ lateral chains, are available as Supporting Information.

The electronic absorption and emission spectra of the macrocycles **1–11** have been studied in methanol, acetonitrile, and nitromethane. The common UV–vis spectral features of these compounds is the observation of two major bands at 250 and around 440 nm due to internal $\pi-\pi^*$ transitions, along with a weak and broad envelop at about 350 nm. The variation of solvents does not have significant effect on the peak positions of the compounds (Table 2), although the absorption intensities are affected more prominently. For the reduced macrocycles **12–22** only a single absorption band of moderate intensity ($\epsilon = 8000\text{--}9000 \text{ M}^{-1}\text{cm}^{-1}$) is observed at ca. 285 nm.

At room temperature, methanol, acetonitrile, or nitromethane solutions of **1–11** on irradiation with light at 440 nm wavelength emit strong to very strong luminescence spectra with their peaks lying between 495 and 510 nm. The excitation spectra of these compounds show features similar to the corresponding absorption spectra. Figure 5 shows the variation of fluorescence intensities of **1–11** in acetonitrile. It may be noted that under similar conditions of measurement, strongest and weakest emission bands are observed for **7** and **3**, respectively. More or less similar trends are observed in methanol and

TABLE 2. Absorption and Emission Spectral Characteristics of Macrocycles **1–11** in Solvents

compd	solvent	absorption		emission ^a	
		λ_{max} , nm (ϵ , M ⁻¹ cm ⁻¹)	λ_{em} , nm	ϕ	
1	methanol	435 (10 500), 250 (35 200)	505	0.073	
	acetonitrile	452 (14 200), 242 (53 000)	508	0.055	
	nitromethane	455 (26 000)	510	0.082	
2	methanol	455 (9500), 245 (29 000)	508	0.069	
	acetonitrile	452 (13 500), 242 (51 100)	510	0.057	
	nitromethane	435 (20 100)	510	0.064	
3	methanol	435 (20 200), 250 (29 800)	508	0.046	
	acetonitrile	435 (23 300), 250 (35 900)	508	0.008	
	nitromethane	435 (26 000)	500	0.024	
4	methanol	425 (13 800), 250 (41 800)	500	0.120	
	acetonitrile	425 (21 300), 250 (45 700)	496	0.074	
	nitromethane	430 (27 700)	497	0.191	
5	methanol	432 (15 800), 250 (36 500)	505	0.054	
	acetonitrile	434 (16 900), 252 (43 000)	500	0.025	
	nitromethane	435 (23 600)	506	0.063	
6	methanol	439 (15 300), 251 (20 150)	501	0.282	
	acetonitrile	437 (26 500), 250 (37 900)	500	0.151	
	nitromethane	437 (29 600)	500	0.233	
7	methanol	437 (19 800), 250 (28 200)	497	0.333	
	acetonitrile	440 (24 700), 251 (36 100)	498	0.221	
	nitromethane	442 (28 500)	498	0.272	
8	methanol	437 (18 100), 250 (28 000)	502	0.202	
	acetonitrile	443 (21 300), 252 (29 900)	498	0.190	
	nitromethane	446 (26 500)	498	0.174	
9	methanol	445 (19 800), 250 (28 800)	500	0.250	
	acetonitrile	445 (22 000), 252 (31 600)	498	0.131	
	nitromethane	447 (30 100)	498	0.243	
10	methanol	442 (18 200), 250 (29 500)	498	0.293	
	acetonitrile	442 (17 300), 250 (28 700)	498	0.172	
	nitromethane	445 (31 500)	498	0.213	
11	methanol	445 (12 400), 251 (36 500)	508	0.081	
	acetonitrile	442 (18 600), 250 (40 100)	510	0.057	
	nitromethane	440 (22500)	510	0.130	
23	acetonitrile	455 (6200), 346 (5900), 238 (39 500)	500 ^b		
24	acetonitrile	450 (7400), 342 (6500), 240 (41 300)	500 ^b		

^a Excitation wavelength 440 nm. ^b Very weak emission.

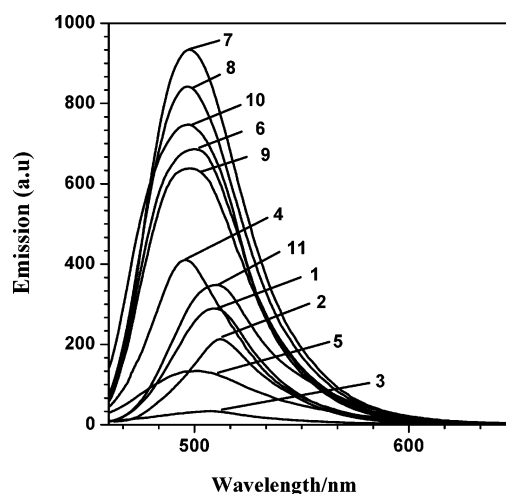


FIGURE 5. Variation of fluorescence intensities of **1–11** in acetonitrile.

acetonitrile. For a given compound, the increased order of fluorescence intensity with respect to solvent is methanol < acetonitrile < nitromethane. The absorption and luminescence characteristics of **1–11** in the three solvents along with the quantum yield of emission (ϕ) are given in Table 2.

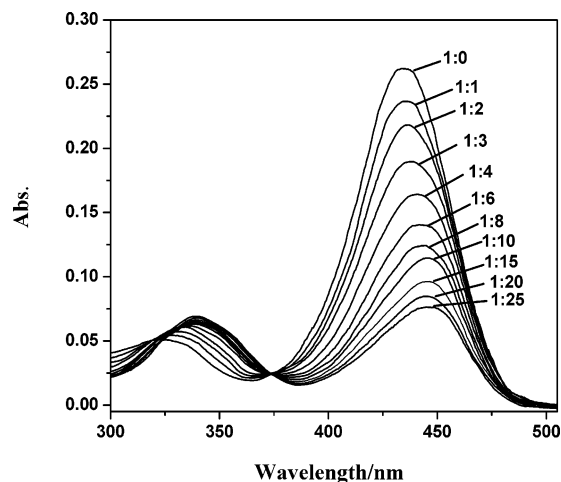


FIGURE 6. Changes in the absorption of **6** (1×10^{-5} M) in acetonitrile with the addition of triethylamine (1×10^{-5} M).

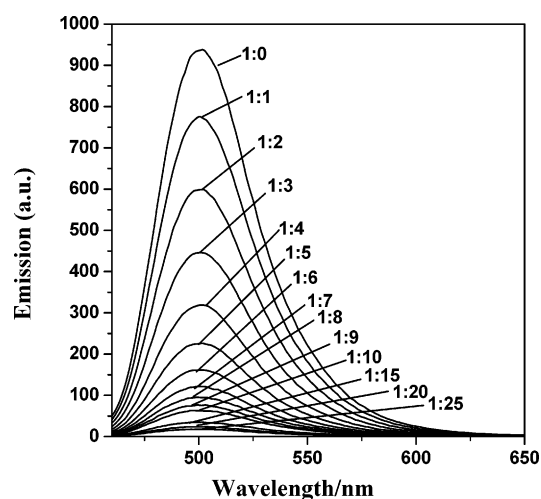
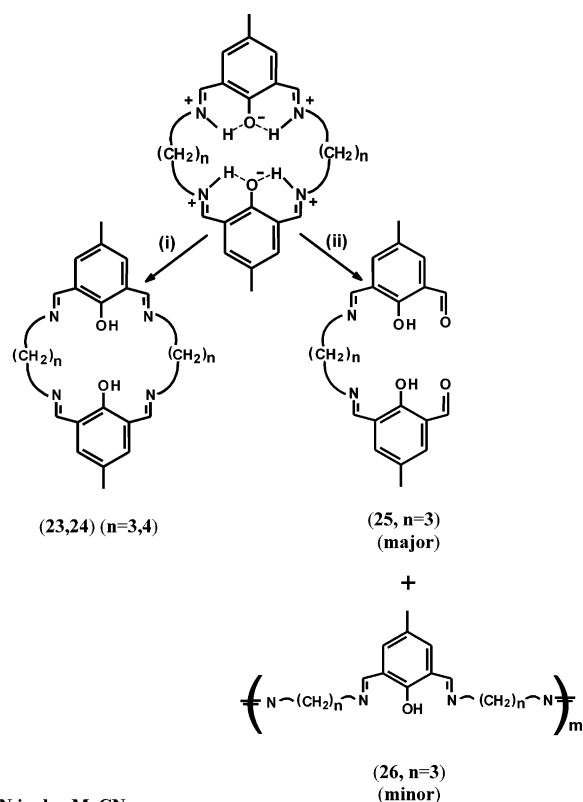


FIGURE 7. Changes in luminescence spectrum of **6** (1×10^{-5} M) in acetonitrile with the addition of triethylamine (1×10^{-5} M).

The effect of addition of a base such as triethylamine to the solution of a $[H_4L](ClO_4)_2$ derivative has been studied both spectrophotometrically and spectrofluorimetrically. Figure 6 shows the changes in absorption of **6** in acetonitrile with the incremental addition of triethylamine. The intensity of the absorption peak of **6** at 437 nm continuously decreases and undergoes a small red shift in position till 25 equiv of triethylamine is added, after which no further change occurs. Simultaneous to the above changes, the growth of a relatively weak band occurs at 342 nm and all the absorption curves pass through an isosbestic point at 375 nm. Complimentary spectrofluorimetric titration behavior observed for **6** is shown in Figure 7. As may be seen, the fluorescence intensity monotonically decreases with the increasing amount of base added. Again, after the addition of 25 equiv no further quenching occurs. Similar observation has been made for the other derivatives also.

To characterize the product formed on treating a $[H_4L](ClO_4)_2$ derivative with excess of triethylamine, the reactions with **3** and **6** were carried out on a preparative scale. The products **23** and **24** (shown in Scheme 2) were obtained as a yellow sticky mass that hardened on

SCHEME 2



- (i) Et_3N in dry MeCN
(ii) 95:5 (v/v) dry MeCN- H_2O mixture

standing. The IR spectra of the compounds showed the absence of perchlorate anions, and the $CH=N$ stretching frequency observed at ca. 1645 cm^{-1} is shifted by $25\text{--}30\text{ cm}^{-1}$ to lower energy compared to the precursors. The compositions of the compounds agreed well with those of the neutral macrocycles H_2L and their 1H NMR spectral data (see Experimental Section) are consistent with the resonance expected for the neutral macrocycles. It should be mentioned, however, that unlike the sharp signals observed for **3** and **6** the resonances observed for **23** and **24** were rather broad. The observations made with **23** and **24** are similar to those reported for the neutral macrocycle H_2L obtained from 4-*tert*-butyl-2,6-diformylphenol and 1,3-diaminopropane using a different synthetic protocol.^{16c} Finally, the dicopper(II) complex $[Cu_2L(H_2O)_2](ClO_4)_2$ prepared from **23** was found to be identical in all respects with the one obtained from **3**. In both cases two reversible redox couples due to $Cu^{II} Cu^{II}/Cu^{II} Cu^I$ and $Cu^{II} Cu^I/Cu^I Cu^I$ were observed in cyclic voltammetric measurements for the copper(II) complexes in dimethyl sulfoxide using glassy carbon electrode with identical $E_{1/2}$ values -0.45 and -0.92 V vs $Ag/AgCl$. Clearly, the macrocycle salts $[H_4L](ClO_4)_2$ on treatment with excess of triethylamine get deprotonated to the neutral macrocycles H_2L . The requirement of excess base indicates the presence of strong intramolecular hydrogen bonding in the salts. The neutral macrocycles H_2L are practically nonluminescent, but with the addition of an acid full recovery of the original luminescence can be achieved. Thus, reversible protonation/deprotonation of the tetraaminodiphenol macrocycles accompanied by manifold increase/decrease in fluorescence is the remarkable characteristic of this class of compounds. By contrast, the

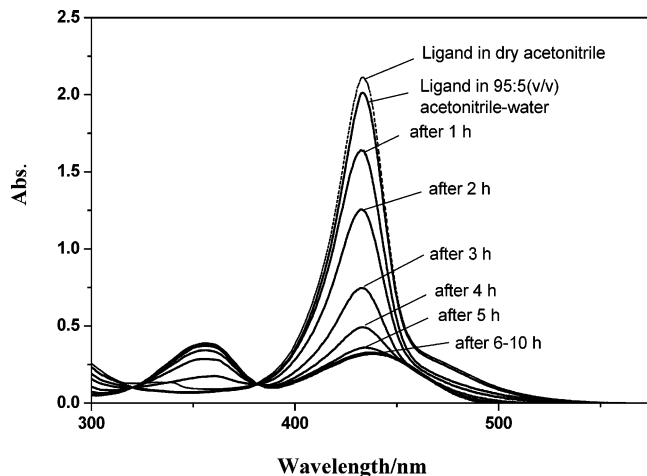


FIGURE 8. Time-dependent absorption spectra of **3** in 95:5 (v/v) acetonitrile–water (9×10^{-5} M).

tetraaminodiphenol macrocycles H_2L' show no luminescence at all.

As already mentioned, the azomethine linkages of the tetraaminodiphenol macrocycles are prone to undergo hydrolytic cleavage. To get an insight of the way the hydrolysis takes place, time-dependent absorption spectra of **3** in 95:5 (v/v) acetonitrile–water has been recorded (Figure 8). It may be noted that over a period of 6 h the intensity of the band at 435 nm steadily decreases with concomitant slow growth of a new band at 360 nm, while the consecutive absorption curves pass through an isosbestic point at 380 nm. The final spectrum is quite similar to that of **25**, the 2:1 condensation product of 4-methyl-2,6-diformylphenol and 1,3-diamine. An additional experiment was carried out by stirring ca. 100 mg of **3** in 20 mL of 1:1 acetonitrile–water for 36 h. The solution was evaporated to dryness on a rotary evaporator, and the residue was extracted with chloroform when the major part went into solution. The undissolved minor portion was treated with acetonitrile, and a spongy solid was isolated from it. The product obtained from the chloroform solution turned out to be **25**. The 1H NMR spectrum of the minor fraction isolated from the acetonitrile solution indicated it to be an oligomeric condensation product (**26**) of 4-methyl-2,6-diformylphenol and 1,3-diaminopropane. It thus appears that when a small amount of water is present in a solvent, the hydrolytic cleavage of $[H_4L](ClO_4)_2$ occurs to the extent of releasing one molecule of diaminoalkane. However, with a larger amount of water, in addition to the above reaction partial release of the dialdehyde and diamines occurs, which in turn undergoes oligomeric condensation reaction.

Conclusion

A remarkably simple and high yield (ca. 90%) synthesis of the dicompartmental tetraaminodiphenol macrocycles $[H_4L](ClO_4)_2$ based on proton-templated [2 + 2] condensation between 4-methyl(*tert*-butyl)-2,6-diformyl(or diacyl)phenols and α,ω -diaminoalkanes is reported in this study. In the one-pot method of synthesis, 1 equiv of diamine is added to a hot methanol solution containing 1 equiv of dialdehyde(or diacyl)phenol, 2 equiv of acetic acid, and 4 equiv of $NaClO_4$, which on standing at room

temperature deposits $[H_4L](ClO_4)_2$ crystals. The novelty of the method is underscored by the fact that C_2 – C_{12} diamines undergo cyclocondensation with equal ease, thus providing easy access to a whole range of 18- to 38-membered tetraaminodiphenol macrocycles. The reduction of these compounds in methanol with $NaBH_4$ followed by dilution of the reaction mixture with water affords corresponding tetraaminodiphenol macrocycles again in a single pot. From structural and spectroscopic studies it has become evident that in $[H_4L](ClO_4)_2$ all four imine nitrogens are protonated and they are intramolecularly hydrogen-bonded to the phenolate oxygens as $N-H \cdots O \cdots H-N$. All of the $[H_4L](ClO_4)_2$ derivatives show strong luminescence at room temperature in methanol, acetonitrile, and nitromethane. The derivative with a C_6 -lateral chain is most fluorescence active. Addition of a base such as triethylamine to the solution of $[H_4L](ClO_4)_2$ causes quenching of fluorescence intensity, although for complete quenching about 25-fold of triethylamine is required. The product isolated under this condition has been characterized to be the macrocycle H_2L in neutral form. The hydrolytic cleavage of the azomethine linkages in $[H_4L](ClO_4)_2$ has been studied with the C_3 -lateral chain derivative. In 9:1 acetonitrile–water mixture, the release of one molecule of 1,3-diaminopropane occurs with the formation of the 1:2 iminoaldehyde derivative. On the other hand, in 1:1 acetonitrile–water mixture, in addition to the above product some diiminophenol oligomeric species also form.

Experimental Section

Synthesis of Tetraaminodiphenol Macrocylic Compounds $[H_4L](ClO_4)_2$ (1–11). General Procedure. A methanol solution (30 mL) containing 4-methyl(or *tert*-butyl)-2,6-diformyl(or diacyl)phenol (2 mmol), $NaClO_4$ (1 g, 8 mmol), and acetic acid (0.25 mL, 4 mmol) was heated to boiling and then slowly treated with a methanol solution (20 mL) of α,ω -diaminoalkane (2 mmol). The solution was removed from the source of heating and kept at room temperature overnight. The product separated as red or orange crystals that were collected by filtration and washed with ethanol and diethyl ether. The filtrate on standing for an additional 24 h provides a second crop of the product, and the combined yield was 90% or more.

Data for 1. IR (KBr; ν in cm^{-1}): 1652s, 1541s, 1223s, 1112s, 628m. 1H NMR (300 MHz, CD_3CN): δ 14.57 (s, 4H); 8.65 (d, $J = 11.0$ Hz, 4H); 7.78 (s, 4H); 4.12 (m, 8H); 2.33 (s, 6H). ^{13}C NMR (75.5 MHz, CD_3CN): δ 170.2, 146.1, 117.7, 51.0, 19.1. Anal. Calcd for $C_{22}H_{26}N_4O_{10}Cl_2$: C, 45.75; H, 4.50; N, 9.71. Found: C, 45.52; H, 4.65; N, 9.65.

Data for 2. IR (KBr; ν in cm^{-1}): 1645s, 1541s, 1226s, 1090s, 627m. 1H NMR (300 MHz, CD_3CN): δ 14.87, 14.73, 14.58, 14.45 (s, 4H); 8.68, 8.65 (dd, $J = 12.5, 11.7$ Hz, 4H); 7.80 (m, 4H); 4.42 (m, 2H); 4.20 (m, 2H); 3.86 (m, 2H); 2.33 (s, 6H); 1.50 (d, 6H). ^{13}C NMR (75.5 MHz, CD_3CN): δ 170.6, 170.4, 167.9, 167.6, 146.5, 146.1, 125.2, 117.5, 56.7, 56.2, 19.2, 15.1. Anal. Calcd for $C_{24}H_{32}N_4O_{11}Cl_2$: C, 46.22; H, 5.13; N, 8.98. Found: C, 46.45; H, 5.03; N, 8.86.

Data for 3. IR (KBr; ν in cm^{-1}): 1660s, 1533s, 1235m, 1110s, 628m. 1H NMR (300 MHz, CD_3CN): δ 13.35 (s, 4H); 8.36 (s, 4H); 7.30 (s, 4H); 4.03 (t, 8H); 2.28 (m, 4H); 2.11 (s, 6H). 1H NMR (300 MHz, $(CD_3)_2SO$): δ 13.17 (s, 4H); 8.57 (d, $J = 13.9$ Hz, 4H); 7.28 (s, 4H); 4.01 (s, 8H); 2.23 (s, 4H); 2.10 (s, 6H). ^{13}C NMR (75.5 MHz, $(CD_3)_2SO$): δ 177.0, 168.5, 146.4, 123.7, 117.5, 52.5, 27.5, 19.8. Anal. Calcd for $C_{24}H_{32}N_4O_{11}Cl_2$: C, 46.22; H, 5.13; N, 8.98. Found: C, 46.46; H, 4.99; N, 9.02.

Data for 4. IR (KBr; ν in cm^{-1}): 1623s, 1527s, 1267m, 1090s, 628m. 1H NMR (300 MHz, $(CD_3)_2SO$): δ 15.32 (s, 4H);

8.08 (s, 4H); 3.93 (s, 8H); 2.74 (s, 12H); 2.32 (s, 6H); 2.20 (m, 4H). ^{13}C NMR (75.5 MHz, $(\text{CD}_3)_2\text{SO}$): δ 178.8, 168.5, 141.2, 123.1, 118.2, 44.2, 29.1, 20.7, 16.6. Anal. Calcd for $\text{C}_{28}\text{H}_{38}\text{N}_4\text{O}_{10}\text{Cl}_2$: C, 50.83; H, 5.74; N, 8.47. Found: C, 51.02; H, 5.86; N, 8.38.

Data for 5. IR (KBr; ν in cm^{-1}): 1655s, 1537s, 1241m, 1097s, 629m. ^1H NMR (300 MHz, $(\text{CD}_3)_2\text{SO}$): δ 13.23 (s, 4H); 8.64 (d, $J = 14.2$ Hz, 4H); 7.58 (s, 4H); 4.00 (s, 8H); 2.28 (s, 4H); 1.13 (s, 18H). ^{13}C NMR (75.5 MHz, $(\text{CD}_3)_2\text{SO}$): δ 176.8, 168.5, 142.6, 136.4, 117.3, 51.3, 30.0, 27.3. Anal. Calcd for $\text{C}_{30}\text{H}_{42}\text{N}_4\text{O}_{10}\text{Cl}_2$: C, 52.25; H, 6.09; N, 8.12. Found: C, 52.01; H, 6.18; N, 7.96.

Data for 6. IR (KBr; ν in cm^{-1}): 1656s, 1536s, 1220s, 1086s, 628m. ^1H NMR (300 MHz, CD_3CN): δ 14.04 (s, 4H); 8.47 (s, 4H); 7.65 (s, 4H); 3.84 (s, 8H); 2.29 (s, 6H); 1.88 (s, 8H). ^{13}C NMR (75.5 MHz, CD_3CN): δ 177.0, 168.9, 146.3, 123.4, 51.9, 27.6, 20.0. Anal. Calcd for $\text{C}_{26}\text{H}_{34}\text{N}_4\text{O}_{10}\text{Cl}_2$: C, 49.29; H, 5.37; N, 8.84. Found: C, 49.04; H, 5.44; N, 8.75.

Data for 7. IR (Nujol; ν in cm^{-1}): 1647s, 1530s, 1093s, 624m. ^1H NMR (300 MHz, CD_3CN): δ 13.80 (s, 4H); 8.37 (d, $J = 13.1$ Hz, 4H); 7.58 (s, 4H); 3.73 (m, 8H); 2.23 (s, 6H), 1.76 (m, 8H); 1.45 (m, 8H). ^{13}C NMR (75.5 MHz, CD_3CN): δ 174.8, 165.7, 143.0, 121.6, 115.3, 49.7, 26.7, 23.6, 16.6. Anal. Calcd for $\text{C}_{30}\text{H}_{44}\text{N}_4\text{O}_{11}\text{Cl}_2$: C, 50.92; H, 6.22; N, 7.92. Found: C, 51.14; H, 6.31; N, 7.88.

Data for 8. IR (KBr; ν in cm^{-1}): 1646s, 1528s, 1226m, 1104s, 627m. ^1H NMR (300 MHz, CD_3CN): δ 13.40 (s, 4H); 8.35 (s, 4H); 7.54 (s, 4H); 3.68 (m, 8H); 2.20 (s, 6H); 1.70 (m, 8H); 1.35 (m, 16H). ^{13}C NMR (75.5 MHz, CD_3CN): δ 175.3, 167.5, 144.7, 123.4, 117.3, 51.7, 28.9, 28.8, 25.7, 18.5. Anal. Calcd for $\text{C}_{34}\text{H}_{52}\text{N}_4\text{O}_{11}\text{Cl}_2$: C, 53.47; H, 6.81; N, 7.34. Found: C, 53.25; H, 6.92; N, 7.47.

Data for 9. IR (KBr; ν in cm^{-1}): 1650s, 1534s, 1224m, 1088s, 624m. ^1H NMR (300 MHz, CD_3CN): δ 13.56 (s, 4H); 8.36 (s, 4H); 7.55 (s, 4H); 3.68 (m, 8H); 2.22 (s, 6H); 1.71 (m, 8H); 1.32 (m, 20H). ^{13}C NMR (75.5 MHz, CD_3CN): δ 176.7, 167.8, 145.2, 123.3, 116.8, 51.6, 28.8, 28.4, 25.8, 18.5. Anal. Calcd for $\text{C}_{36}\text{H}_{60}\text{N}_4\text{O}_{12}\text{Cl}_2$: C, 53.40; H, 7.17; N, 6.92. Found: C, 53.76; H, 7.14; N, 6.99.

Data for 10. IR (Nujol; ν in cm^{-1}): 1650s, 1537s, 1235m, 1087s, 622m. ^1H NMR (300 MHz, CD_3CN): δ 13.68 (s, 4H); 8.37 (s, 4H); 7.55 (s, 4H); 3.70 (m, 8H); 2.23 (s, 6H); 1.73 (m, 12H); 1.36–1.26 (m, 28H). ^{13}C NMR (75.5 MHz, CD_3CN): δ 176.2, 167.6, 144.9, 117.2, 51.5, 29.0, 28.6, 25.8, 18.5. Anal. Calcd for $\text{C}_{42}\text{H}_{68}\text{N}_4\text{O}_{11}\text{Cl}_2$: C, 57.60; H, 7.77; N, 6.40. Found: C, 57.84; H, 7.73; N, 6.48.

Data for 11. IR (KBr; ν in cm^{-1}): 1654s, 1536s, 1230m, 1089s, 628m. ^1H NMR (300 MHz, CD_3CN): δ 14.60 (s, 4H); 8.65 (d, $J = 13.3$ Hz, 4H); 7.82 (s, 4H); 3.87 (d, $J = 9.9$ Hz, 4H); 2.33 (s, 6H); 2.08 (m, 8H); 1.50 (m, 28H). ^{13}C NMR (75.5 MHz, $(\text{CD}_3)_2\text{SO}$): δ 175.0, 165.2, 145.0, 121.6, 116.2, 60.6, 25.3, 22.3, 18.4. Anal. Calcd for $\text{C}_{30}\text{H}_{40}\text{N}_4\text{O}_{11}\text{Cl}_2$: C, 51.20; H, 5.68; N, 7.96. Found: C, 50.94; H, 5.76; N, 8.02.

Synthesis of Tetraaminodiphenol Macrocylic Compounds $\text{H}_2\text{L}'$ (12–22). General Procedure. To a stirred methanol (30 mL) suspension of $[\text{H}_4\text{L}](\text{ClO}_4)_2$ (0.5 mmol) was added solid NaBH_4 (0.5 g, ca. 13 mmol) in small portions. The solid material gradually went into solution, and ultimately an almost colorless solution was obtained over a period of 0.5 h. This was filtered, and to the filtrate was added slowly 30 mL of water with stirring, and the resulting solution was allowed to stand overnight, during which period the product separated out as white crystals. The product was collected by filtration and recrystallized from methanol–water. The yield varies from 40% to 60%.

In the cases of **14** and **16** the products were isolated in a different way. After reduction the methanol solution was diluted with 100 mL of water and acidified with HCl (4 M). The solution was filtered, the pH of the solution was brought to ca. 10 with aqueous ammonia, and then the solution was extracted with CH_2Cl_2 (3×70 mL). The organic layer was

dried over Na_2SO_4 and then evaporated to dryness. The residue was extracted with 80–100 °C petroleum ether on a Soxhlet apparatus and the extract on cooling at 0 °C deposited a white crystalline product.

Data for 12. IR (KBr; ν in cm^{-1}): 3338w, 3268s, 1611m, 1450s. ^1H NMR (300 MHz, CDCl_3): δ 6.79 (s, 4H); 3.82 (s, 8H); 2.82 (s, 8H); 2.20 (s, 6H). ^{13}C NMR (75.5 MHz, CDCl_3): δ 154.6, 129.5, 128.7, 128.0, 125.0, 52.3, 48.9, 20.8. Anal. Calcd for $\text{C}_{22}\text{H}_{32}\text{N}_4\text{O}_2$: C, 68.75; H, 8.33; N, 14.60. Found: C, 68.89; H, 8.21; N, 14.48. Mp: 220 °C.

Data for 13. IR (KBr; ν in cm^{-1}): 3326m, 3190m, 1610m, 1483s. ^1H NMR (300 MHz, CDCl_3): δ 6.84 (s, 2H); 6.78 (s, 2H); 3.85, 3.83, 3.78, 3.73 (s, 8H); 2.85 (m, 2H); 2.75 (m, 2H); 2.60 (m, 2H); 2.21 (s, 6H); 1.14 (d, $J = 6.1$ Hz, 6H). ^{13}C NMR (75.5 MHz, CDCl_3): δ 154.6, 129.9, 129.0, 128.1, 125.5, 124.2, 56.3, 53.1, 49.6, 20.7, 18.4. Anal. Calcd for $\text{C}_{24}\text{H}_{36}\text{N}_4\text{O}_2$: C, 69.69; H, 8.73; N, 13.59. Found: C, 69.46; H, 8.81; N, 13.50. Mp: 202 °C.

Data for 14. IR (KBr; ν in cm^{-1}): 3313m, 3261m, 1609m, 1475s. ^1H NMR (300 MHz, CDCl_3): δ 6.72 (s, 4H); 3.84 (s, 8H); 3.30 (br, 6H); 2.56 (t, 8H); 2.18 (s, 6H); 1.70 (m, 4H). ^{13}C NMR (75.5 MHz, CDCl_3): δ 154.4, 128.8, 127.0, 124.0, 51.2, 46.5, 29.8, 20.1. Anal. Calcd for $\text{C}_{24}\text{H}_{36}\text{N}_4\text{O}_2$: C, 69.69; H, 8.73; N, 13.59. Found: C, 69.58; H, 8.67; N, 13.69. Mp: 144 °C.

Data for 15. IR (KBr; ν in cm^{-1}): 3313m, 3270s, 1608m, 1475s. ^1H NMR (300 MHz, CDCl_3): δ 6.77, 6.76, 6.74, 6.73 (s, 4H); 3.92 (m, 4H); 3.32 (br, 6H); 2.63 (m, 8H); 2.21 (s, 6H); 1.70 (m, 4H); 1.42 (m, 2H). ^{13}C NMR (75.5 MHz, CDCl_3): δ 153.1–152.7 (multiple lines), 128.0–126.9 (multiple lines), 57.6–56.1 (multiple lines), 46.7–45.6 (multiple lines), 28.6–28.2 (multiple lines), 22.0–21.4 (multiple lines), 20.5. Anal. Calcd for $\text{C}_{28}\text{H}_{44}\text{N}_4\text{O}_2$: C, 71.79; H, 9.40; N, 11.97. Found: C, 71.54; H, 9.49; N, 12.04. Mp: 102 °C.

Data for 16. IR (KBr; ν in cm^{-1}): 3298w, 3262m, 1613m, 1474s. ^1H NMR (300 MHz, CDCl_3): δ 6.94 (s, 4H); 4.12 (br, 6H); 3.86 (s, 8H); 2.67 (t, 8H); 1.75 (m, 4H); 1.24 (s, 18H). ^{13}C NMR (75.5 MHz, CDCl_3): δ 154.3, 141.0, 125.1, 123.3, 51.8, 46.6, 33.8, 31.4, 29.7. Anal. Calcd for $\text{C}_{30}\text{H}_{48}\text{N}_4\text{O}_2$: C, 70.58; H, 9.68; N, 11.29. Found: C, 72.45; H, 9.76; N, 11.16. Mp: 117 °C.

Data for 17. IR (KBr; ν in cm^{-1}): 3308w, 3271m, 1616m, 1477s. ^1H NMR (300 MHz, CDCl_3): δ 6.78 (s, 4H); 3.82 (s, 8H); 2.62 (s, 8H); 2.20 (s, 6H); 1.57 (s, 8H). ^{13}C NMR (75.5 MHz, CDCl_3): δ 154.8, 129.4, 127.9, 124.6, 51.9, 49.0, 27.9, 20.8. Anal. Calcd for $\text{C}_{26}\text{H}_{40}\text{N}_4\text{O}_2$: C, 70.91; H, 9.09; N, 12.73. Found: C, 71.14; H, 8.89; N, 12.67. Mp: 176 °C.

Data for 18. IR (KBr; ν in cm^{-1}): 3310m, 3264m, 1615m, 1477s. ^1H NMR (300 MHz, CDCl_3): δ 6.79 (s, 4H); 3.83 (s, 8H); 2.60 (t, 8H); 2.21 (s, 6H); 1.50 (m, 8H); 1.34 (m, 8H). ^{13}C NMR (75.5 MHz, CDCl_3): δ 154.2, 128.7, 127.4, 124.3, 51.4, 48.6, 29.6, 26.9, 20.3. Anal. Calcd for $\text{C}_{30}\text{H}_{48}\text{N}_4\text{O}_2$: C, 72.58; H, 9.68; N, 11.29. Found: C, 72.26; H, 9.80; N, 11.29. Mp: 194 °C.

Data for 19. ^1H NMR (300 MHz, CDCl_3): δ 6.79 (s, 4H); 3.85 (s, 8H); 3.20 (br, 6H); 2.62 (t, 8H); 2.21 (s, 6H); 1.50 (m, 8H); 1.29 (m, 16H). ^{13}C NMR (75.5 MHz, CDCl_3): δ 154.3, 128.8, 127.4, 123.8, 51.3, 48.6, 29.5, 29.2, 26.9, 20.3. Anal. Calcd for $\text{C}_{34}\text{H}_{56}\text{N}_4\text{O}_2$: C, 73.91; H, 10.14; N, 10.12. Found: C, 74.11; H, 10.21; N, 9.99. Mp: 240 °C.

Data for 20. IR (KBr; ν in cm^{-1}): 3318w, 3268m, 1612m, 1476s. ^1H NMR (300 MHz, CDCl_3): δ 6.72 (s, 4H); 4.35 (br, 6H); 3.76 (s, 8H); 2.53 (m, 8H); 2.13 (s, 6H); 1.43 (m, 8H); 1.20 (m, 8H). ^{13}C NMR (75.5 MHz, CDCl_3): δ 154.2, 128.7, 127.3, 123.8, 51.3, 48.8, 29.4, 27.0, 20.3. Anal. Calcd for $\text{C}_{36}\text{H}_{60}\text{N}_4\text{O}_2$: C, 74.48; H, 10.34; N, 9.66. Found: C, 74.14; H, 10.50; N, 9.78. Mp: 117 °C.

Data for 21. ^1H NMR (300 MHz, CDCl_3): δ 6.80 (s, 4H); 3.83 (s, 8H); 3.18 (br, 6H); 2.65 (t, 8H); 2.21 (s, 6H); 1.50 (m, 8H); 1.25 (m, 32H). ^{13}C NMR (75.5 MHz, CDCl_3): δ 154.2, 128.6, 127.3, 123.9, 51.2, 50.7, 48.9, 29.4, 27.4, 20.3. Anal. Calcd for $\text{C}_{42}\text{H}_{72}\text{N}_4\text{O}_2$: C, 75.90; H, 10.84; N, 8.43. Found: C, 76.36; H, 10.98; N, 8.28. Mp: 81 °C.

Data for 22. IR (KBr; ν in cm^{-1}): 3305w, 3267m, 1612w, 1477s. ^1H NMR (300 MHz, CDCl_3): δ 6.76 (s, 4H); 3.94 (d, $J = 12.6$ Hz, 4H); 3.66 (d, $J = 12.3$ Hz, 4H); 2.27 (m, 8H); 2.20 (s, 6H); 1.76 (m, 4H); 1.24 (m, 4H); 1.04 (m, 4H). ^{13}C NMR (75.5 MHz, CDCl_3): δ 154.3, 129.2, 127.3, 124.3, 60.4, 48.8, 30.8, 24.7, 20.2. Anal. Calcd for $\text{C}_{30}\text{H}_{44}\text{N}_4\text{O}_2$: C, 73.17; H, 8.94; N, 11.38. Found: C, 72.83; H, 9.06; N, 11.27. Mp: 230 °C.

Conversion of $[\text{H}_4\text{L}](\text{ClO}_4)_2$ to H_2L (23, 24). General Procedure. To a stirred acetonitrile solution (30 mL) of $[\text{H}_4\text{L}](\text{ClO}_4)_2$ (0.5 mmol) was added triethylamine (1.26 g, 12.5 mmol) over a period of 0.5 h when the solution become cloudy, and eventually an amorphous yellow mass precipitated. After 1 h, the product was filtered off and washed thoroughly first with methanol and with diethyl ether.

Data for 23. IR (Nujol; ν in cm^{-1}): 1630s. ^1H NMR (300 MHz, CDCl_3): δ 13.88 (s, 2H); 8.47 (s, 4H); 7.19 (s, 4H); 3.65 (s, 8H); 2.20 (s, 6H); 2.04 (s, 4H). Anal. Calcd for $\text{C}_{24}\text{H}_{28}\text{N}_4\text{O}_2$: C, 71.29; H, 6.93; N, 13.86. Found: C, 70.91; H, 6.79; N, 13.72.

Data for 24. IR (Nujol; ν in cm^{-1}): 1630s. ^1H NMR (300 MHz, CDCl_3): δ 13.92 (s, 2H); 8.48 (s, 4H); 7.35 (s, 4H); 3.58 (s, 8H); 2.21 (s, 6H); 1.72 (s, 8H). Anal. Calcd for $\text{C}_{26}\text{H}_{32}\text{N}_4\text{O}_2$: C, 72.22; H, 7.41; N, 12.96. Found: C, 72.59; H, 7.49; N, 12.88.

Hydrolysis of $[\text{H}_4\text{L}](\text{ClO}_4)_2$. The experiment carried out with **3** is typical of the series. A solution (30 mL) of **3** (200 mg) in 1:1 acetonitrile–water was stirred for 36 h. The solution was evaporated to dryness, and the residue was extracted with chloroform when major part of the solid went into solution. The orange-colored solid (**25**) crystallized out from the chloroform solution gave the composition $\text{C}_{21}\text{H}_{22}\text{N}_2\text{O}_4$. Mp 179 °C. ^1H NMR (300 MHz, CDCl_3): δ 14.13 (s, 2H); 10.42 (s, 2H); 8.33 (s, 2H); 7.23 (d, $J = 11.9$ Hz, 4H); 3.70 (s, 4H); 2.24 (s, 6H).

The chloroform insoluble yellow fraction (**26**) was washed with methanol and dried in air. ^1H NMR (300 MHz, CD_3CN): δ 8.31 (s, 2H); 7.26 (s, 2H); 3.99 (s, 4H); 2.08 (s, 3H).

X-ray Crystallography. The crystal structure analyses were carried out for compounds **1** and **6**. The intensity data were collected at 203 K using graphite-monochromated Mo $K\alpha$ radiation ($\lambda = 0.71073$ Å) in ω -scan mode. The intensity data were corrected for Lorentz-polarization effects and semiempirical absorption corrections were made from ψ -scans. The structures were solved by direct and Fourier methods and refined by full-matrix least-squares based on F^2 using the SHELXTL software package.²⁶ The nonhydrogen atoms were refined anisotropically, while the hydrogen atoms attached to the carbon atoms were fixed at the geometrically calculated

positions with fixed isotropic thermal parameters. The hydrogen atoms bonded to the nitrogen/oxygen atoms were refined free.

Data for 1. $\text{C}_{22}\text{H}_{26}\text{Cl}_2\text{N}_4\text{O}_{10}$, MW = 577.37, monoclinic, space group C_2 , $a = 17.421(3)$, $b = 14.720(2)$, $c = 20.772(4)$ Å, $\alpha = 90^\circ$, $\beta = 107.49(1)^\circ$, $\gamma = 90^\circ$, $V = 5080.5(15)$ Å³, $Z = 8$, $\theta = 2.45$ – 27.00° , measd reflns = 6185, independent reflns = 6100. Final R indices [$I > 2\sigma(I)$]: $R1 = 0.0870$, $wR2 = 0.1433$. R (all data): $R1 = 0.2197$, $wR2 = 0.1905$.

Data for 6. $\text{C}_{26}\text{H}_{34}\text{Cl}_2\text{N}_4\text{O}_{10}$, MW = 633.47, triclinic, space group $P-1$, $a = 7.655(5)$, $b = 8.912(4)$, $c = 11.204(12)$ Å, $\alpha = 94.63(9)^\circ$, $\beta = 100.47(9)^\circ$, $\gamma = 106.95(4)^\circ$, $V = 711.7(9)$ Å³, $Z = 1$, $\theta = 2.83$ – 27.50° , measd refln = 3485, independent refln = 3245. Final R indices [$I > 2\sigma(I)$]: $R1 = 0.0735$, $wR2 = 0.1791$. R (all data): $R1 = 0.1321$, $wR2 = 0.2489$.

Detailed X-ray crystallographic data for **1** and **6** are available in CIF format as Supporting Information.

Emission Quantum Yield. Quantum yields of compounds **1**–**11** were measured at room temperature for their methanol, acetonitrile, and nitromethane solutions relative to perylene as the standard.²⁷ The quantum yields were calculated using the relation²⁸

$$\varphi = \varphi_{\text{std}} \left(\frac{A_{\text{std}}}{A} \right) \left(\frac{I}{I_{\text{std}}} \right) \left(\frac{\eta^2}{\eta_{\text{std}}^2} \right)$$

where A , I , and η refer to absorbance, integrated emission intensity, and solution refractive index, respectively.

CAUTION: The perchlorate salts used in this study are potentially explosive and should be handled with care.

Supporting Information Available: General experimental procedure; ^1H NMR spectra for compounds **2**, **7**, **9**, **15**, **19**, and **21**; optimized configurations for compounds **12**–**22**; and X-ray crystallographic data for compounds **1** and **6** in CIF format. This material is available free of charge via the Internet at <http://pubs.acs.org>.

JO049787S

(26) Sheldrick, G. M. *SHELXTL97-2*, Program for the Refinement of Crystal Structures; University of Göttingen: Göttingen, Germany, 1997.

(27) Du, H.; Fuh, R. A.; Li, J.; Corkan, A.; Lindsay, J. S. *Photochem. Photobiol.* **1998**, *68*, 141.

(28) Van Houten, J.; Watts, R. J. *J. Am. Chem. Soc.* **1976**, *98*, 4853.